Proceedings of the 17th World Congress
The International Federation of Automatic Control
Seoul, Korea, July 6-11, 2008

Design of Disturbance Observer via the Robust Stabilization and H_∞ Loop Shaping Methods

Jun Moon*, Choong Woo Lee*, Chung Choo Chung†, and Young Sik Kim*****

**Division of Electrical and Computer Engineering, Hanyang University, Seoul 133-791, KOREA*
(e-mail: junmoony@gmail.com, choongwoo73@yahoo.co.kr).
*** Division of Electrical and Biomedical Engineering, Hanyang University, Seoul 133-791, KOREA*
(Tel: +82-2220-1724, ;e-mail: cchung@hanyang.ac.kr).
**** LG Electronics Institute of Technology, Seoul 137-724, KOREA*
(e-mail:ysrevol@lge.com).

Abstract: The Disturbance observer (DOB) method is known to be effective in enhancing the performance of dynamic systems in the presence of disturbances. DOBs of various structures have been proposed to improve systems' sensitivity functions for better disturbance rejection performance and robustness. However, the improvement to the sensitivity function may deteriorate robustness and transient responses. In this paper, we propose a new systematic method of designing the DOB. This method is based on the robust stabilization of the normalized coprime factor plant description and H_∞ loop shaping method. In our method, good system robustness can be achieved by Nehari stability margin, and the design parameters of the Q-filter for system robustness and performance can be determined systematically using a target loop transfer function. We applied this method to a MEMS stage. Simulation results show that the disturbance effect of the stage is reduced, and a robust system is achieved in the presence of parameter uncertainties.

1. INTRODUCTION

Disturbance observer (DOB) is known to be an effective method to compensate for the disturbance of a motion control system. Since DOB was proposed (Ohnishi, 1987), the definition of disturbance has been expanded to include the parameter uncertainties and internal disturbances (Ohishi et al., 1988). The purpose of using DOB is to enhance the performance of the systems by observing and eliminating these undesirable disturbances (Unemo et al., 1993). However DOB may cause poor robustness and transient responses because of an increased peak of the sensitivity function. In DOB, the disturbance rejection performance depends on the Q-filter's (low pass filter) order. Its robustness also depends on the relative degree and denominator order of the Q-filter (Choi et al., 2003).

Various methods have been developed for the design of DOB. For system robustness, doubly coprime factorization and Youla-parameterization are used to design robust DOB in the presence of plant input multiplicative uncertainty (Ohishi et al., 1996). In another method, DOB is treated as a controller with two degrees of freedom, and is designed using sensitivity and complementary sensitivity function optimization (Unemo et al., 1993). The robust internal-loop compensator (RIC) method is also a robust DOB (Kim et al., 2002). In this method, the Q-filter is systematically determined by the reference model and the desired feedback controller, but its design is constrained by the type of feedback controller used. To improve disturbance rejection performance, several types of DOB have been proposed. The high order DOB can achieve a rapid transient response and low sensitivity to disturbances (Yamada et al., 1996; Komada et al., 2000), but can have low damping characteristics due to large phase lag. Another approach is error based DOB (EDOB), which is a modified DOB that doesn't use additional sensors to measure the reference input (Yang et al., 2002). Besides these methods, six design guidelines for DOB are proposed to improve system robustness and performance for second order systems only (Choi et al., 2003). In all of these methods, we still have to determine the design parameters of the Q-filter, such as time constant and filter order, to achieve better disturbance rejection and system robustness. The use of trial and error in determining the parameters and order of the Q-filter is inevitable.

In this paper, we propose a new systematic design method of the DOB Q-filter. This method is based on the stabilization of the normalized coprime factor plant description (Glover et al., 1989) and the H_∞ loop shaping method (McFarlane et al., 1992). In this method, DOB guarantees robust stability by a Nehari optimal stability margin (Glover et al., 1989). Also the parameters and order of the Q-filter required to achieve system robustness and performance are determined systematically by the desired target loop transfer function (McFarlane et al., 1992).

We apply this proposed DOB to a Micro-Electro-Mechanical Systems (MEMS) stage. In this system, the output disturbances are considered to be the stage coupling dynamics and the low frequency noise component which may affect the position of the MEMS stage during tracking operations. Parameter uncertainties such as a variation in

†*Corresponding author*. e-mail: cchung@hanyang.ac.kr

resonance frequency and the damping ratio are also critical problems for system robustness and performance. Simulation results show that disturbances to the MEMS stage are reduced by the proposed DOB. Also, high system robustness is achieved in the presence of parameter uncertainties.

This paper is structured in the following way. In Section 2, the robust stabilization of DOB and the H_∞ loop shaping DOB are detailed. In Section 3, we illustrate the control system design for the MEMS stage. In Section 4, we show the simulation results of the proposed method. In Section 5, we conclude the paper.

2. H_∞ LOOP SHAPING DESIGN OF DOB

The robust stabilization of normalized coprime factor plant description and the H_∞ loop shaping method were proposed by Glover and McFarlane (Glover et al., 1989; McFarlane et al., 1992). In this paper we use these methods to describe the new design procedure for DOB. The following sub-sections include a summary of those methods.

2.1 Robust Stabilization of DOB

Coprime uncertainty model is presented in Fig. 1(a). In this figure, the signal, u, is a control input, δ is the disturbance, y is the output, η is the sensor noise, φ is the output signal from the perturbation, and z_1 and z_2 are the input signals to the perturbation. Let the nominal plant model have normalized coprime factorizations, $\tilde{N}$ and $\tilde{M}^{-1}$, such that

$$G = \tilde{M}^{-1}\tilde{N} . \tag{1}$$

Then the perturbed plant model can be written as

$$G_\Delta = \left(\tilde{M} + \Delta_{\tilde{M}}\right)^{-1}\left(\tilde{N} + \Delta_{\tilde{N}}\right) \tag{2}$$

where $\Delta_{\tilde{N}}$ and $\Delta_{\tilde{M}}$ are stable proper transfer functions which represent the uncertainty in the nominal plant model. $\Delta_{\tilde{M}}$ can be represented as the low frequency plant parameter uncertainty, while $\Delta_{\tilde{N}}$ can be represented as the high frequency unmodeled dynamics (Vinnicombe, 2001).

The object of robust stabilization is to stabilize not only the nominal plant model, G, but also a family of perturbed plants defined by

$$G_P = \left\{\left(\tilde{M} + \Delta_{\tilde{M}}\right)^{-1}\left(\tilde{N} + \Delta_{\tilde{N}}\right) : \left\|\begin{bmatrix}\Delta_{\tilde{M}} & \Delta_{\tilde{N}}\end{bmatrix}\right\|_\infty < \varepsilon\right\} \tag{3}$$

where $\varepsilon > 0$ is the stability margin. The perturbed feedback system from φ to z_1 and z_2 in Fig. 1(a) is robust stable if and only if

$$\left\|\begin{bmatrix}K_{DOB} \\ I\end{bmatrix}\left(I - GK_{DOB}\right)^{-1}\tilde{M}^{-1}\right\|_\infty \le \frac{1}{\varepsilon} = \gamma . \tag{4}$$

The maximum stability margin, $\varepsilon_{\max}$, is given by

$$1/\varepsilon_{\max} = \gamma_{\min} = \left\{1 - \left\|\begin{bmatrix}\tilde{M} & \tilde{N}\end{bmatrix}\right\|_H^2\right\}^{-1/2} = \left(1 + \rho\left(XZ\right)\right)^{1/2} . \tag{5}$$

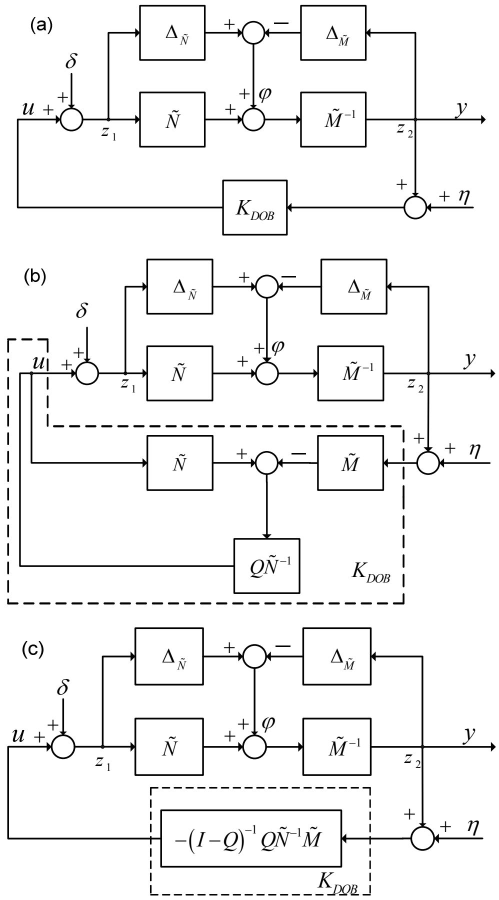

Fig. 1. Robust stabilization of DOB, (a) Coprime uncertainty description, (b) DOB represented by coprime factors and uncertainties, (c) Equivalent form of (b)

In (5), $\|\cdot\|_H$ denotes the Hankel norm, ρ denotes the spectral radius (maximum eigenvalue), and X and Z are the solutions of two Riccati equations (6) for the state space realization (A,B,C,D) of G (Skogestad et al., 2005).

$$\begin{aligned}
&\left(A - BS^{-1}D^TC\right)Z + Z\left(A - BS^{-1}D^TC\right)^T - ZC^TR^{-1}CZ + BS^{-1}B^T = 0 \\
&\left(A - BS^{-1}D^TC\right)^T X + X\left(A - BS^{-1}D^TC\right) - XBS^{-1}B^TX + C^TR^{-1}C = 0 \\
&R = I + DD^T,\;\; S = I + D^TD
\end{aligned} \tag{6}$$

In (Choi et al. 2003), the parameters of the Q-filter are determined from the given second order nominal plant. In this paper, we present a different approach. In Fig. 1(b), the control input, u, can be computed using (7). The diagram in Fig. 1(b) can be rearranged to give the equivalent form seen in Fig. 1(c).

$$\begin{aligned}
u &= K_{DOB}(y + \eta) \\
&= Q\tilde{N}^{-1}\left(\tilde{N}u - \tilde{M}(y + \eta)\right) \\
&= Qu - Q\tilde{N}^{-1}\tilde{M}y - Q\tilde{N}^{-1}\tilde{M}\eta \\
&= -\left(I - Q\right)^{-1}Q\tilde{N}^{-1}\tilde{M}(y + \eta)
\end{aligned} \tag{7}$$

Then the robust stabilization controller, K_{DOB}, can be defined by

$$K_{DOB} = -\left(I - Q\right)^{-1}Q\tilde{N}^{-1}\tilde{M} . \tag{8}$$

From (8), the DOB Q-filter can be expressed as

$$Q = K_{DOB}\left(K_{DOB} - \tilde{N}^{-1}\tilde{M}\right)^{-1}. \tag{9}$$

Therefore, given the nominal coprime factor plant description, the DOB Q-filter can be obtained using the robust stabilization controller, K_{DOB}. Furthermore, K_{DOB}, will be designed by the H$_\infty$ loop shaping method in Section 2.2. As in (4), the robust stabilization of DOB can be written as follows.

Proposition 1: The Robust Stabilization of DOB

DOB represented by the coprime factor is robust stable for all allowed perturbations with $\left\|\begin{bmatrix}\Delta_{\tilde{M}} & \Delta_{\tilde{N}}\end{bmatrix}\right\|_\infty < \varepsilon$, if and only if

$$\begin{aligned}&\left\|\begin{bmatrix}K_{DOB} \\ I\end{bmatrix}(I - GK_{DOB})^{-1}\tilde{M}^{-1}\right\|_\infty \\ &= \left\|\begin{bmatrix}-(I-Q)^{-1}Q\tilde{N}^{-1}\tilde{M} \\ I\end{bmatrix}\left(I - G\left(-(I-Q)^{-1}Q\tilde{N}^{-1}\tilde{M}\right)\right)^{-1}\tilde{M}^{-1}\right\|_\infty \le \frac{1}{\varepsilon} = \gamma\end{aligned}.$$

Proof: This proposition can be proved based on the small gain theorem (Zhou, 1998).

If System 1 is an SISO system, then (9) can be modified as

$$Q = -K_{DOB}G\left(1 - K_{DOB}G\right)^{-1}. \tag{10}$$

From (10), Proposition 1 can be modified for the SISO system.

Proposition 2: If the system in (1) is an SISO system, then DOB represented by the coprime factor is robust stable for all allowed perturbations with $\left\|\begin{bmatrix}\Delta_{\tilde{M}} & \Delta_{\tilde{N}}\end{bmatrix}\right\|_\infty < \varepsilon$, if and only if

$$\left\|\begin{bmatrix}K_{DOB} \\ 1\end{bmatrix}\left(1 - GK_{DOB}\right)^{-1}\tilde{M}^{-1}\right\|_\infty = \left\|\begin{bmatrix}-QG^{-1} & -Q \\ (1-Q) & (1-Q)G\end{bmatrix}\right\|_\infty \le \frac{1}{\varepsilon} = \gamma.$$

Proof: See Appendix A.

From Proposition 2, given an SISO plant model, G, and a DOB Q-filter from (9), we can estimate the allowable maximum bound of the coprime factor uncertainties, $\Delta_{\tilde{N}}$ and $\Delta_{\tilde{M}}$.

2.2 DOB Design Procedure using the H$_\infty$ Loop Shaping Method

In Section 2.1 our goal was to find the robust stabilization controller, K_{DOB}, to satisfy Proposition 1. In this section, we introduce the design procedure for K_{DOB} using the H$_\infty$ loop shaping method illustrated in Fig. 2. The advantage of this method is that we can design a robust K_{DOB} if the following condition is satisfied.

Design Procedure:

① Design DOB's desired loop transfer function, L_{DOB}.

② From L_{DOB}, determine the pre- and post-filters, W_{DOB1} and W_{DOB2}.

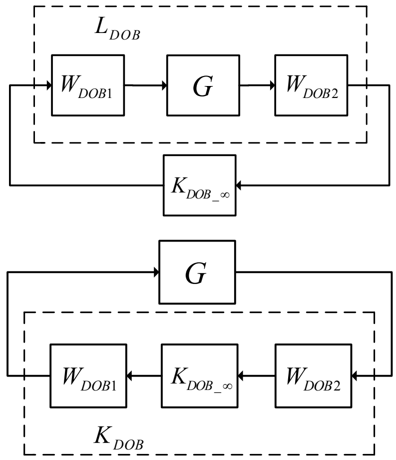

Fig. 2. H$_\infty$ loop shaping design procedure

③ Determine the maximum stability margin, $\varepsilon_{\max}$, of DOB using (5).

If the maximum stability margin is too small, return to Step 2 and modify the pre- and post-filters. Otherwise, select γ to be greater than $\gamma_{\min}$ by about 10% to synthesize the sub-optimal control (Skogestad et al., 2005).

④ Design the H$_\infty$ loop shaping controller, K_{DOB_∞}, using

$$\begin{aligned}K_{DOB\_\infty} &= \left[\begin{array}{c|c}A + BF + H(C + DF) & H \\ \hline B^T X & -D^T\end{array}\right] \\ F &= -S^{-1}(D^T C + B^T X) \\ L &= (1-\gamma^2)I + XZ \qquad (\gamma = 1/\varepsilon) \\ H &= \gamma^2 (L^T)^{-1} Z C^T\end{aligned}.$$

⑤ Use $K_{DOB} = W_{DOB1}K_{DOB\_\infty}W_{DOB2}$ to design the controller K_{DOB}.

⑥ Design the Q-filter using (9).

3. CASE STUDY

In this section, we design the track following control system by applying the proposed DOB to a MEMS stage used in scanning-probe data storage systems. The goal of the track following control for the probe storage system is for the position of MEMS stage to be maintained on the track center line in the presence of disturbances and model parameter uncertainties. In this paper, we consider only the x-axis which keeps the stage positioned on the track center line during the scanning operation (Pantazi et al., 2007). The modelling equation for the MEMS stage is

$$G_x(s) = \frac{k\omega_n^2}{s^2 + 2\varsigma\omega_n s + \omega_n^2} \tag{11}$$

where the damping ratio, ς, is 0.0035, the natural frequency, ω_n, is 510.5 rad/s, and DC gain, k, is 7.708. This MEMS stage is fabricated by LG Electronics.

Figure 3 shows the close loop control structure. In this figure, G_x is the x-axis model of the MEMS stage, K_x is the feedback controller and K_{DOB} is the proposed DOB controller. We design both K_x and K_{DOB} using the H_∞ loop shaping method. Hence we can design K_x and K_{DOB} simultaneously by constructing the transfer function matrix.

The transfer functions of the desired loop transfer functions, pre- and post-filters are shown in (12) and (13).

$$G_s = W_2 G W_1 = \begin{bmatrix} L_{DOB} & 0 \\ 0 & L_x \end{bmatrix}$$
$$G = \begin{bmatrix} G_x & 0 \\ 0 & G_x \end{bmatrix} \quad W_1 = \begin{bmatrix} W_{DOB1} & 0 \\ 0 & W_{x1} \end{bmatrix} \quad W_2 = \begin{bmatrix} W_{DOB2} & 0 \\ 0 & W_{x2} \end{bmatrix} \tag{12}$$

$$W_{DOB1} = \frac{(4.5\times10^5)s^2 + (1.6\times10^7)s + (1.1\times10^{11})}{(1.8\times10^6)s^2 + (1.4\times10^9)s + (4.6\times10^{11})}$$
$$W_{DOB2} = 1$$
$$W_{x1} = \frac{(1.3\times10^4)s^3 + (1.7\times10^{11})s^2 + (6.2\times10^{12})s + (4.5\times10^{16})}{s^4 + (1.2\times10^7)s^3 + (2.1\times10^{11})s^2 + (4.5\times10^{14})s + (4.5\times10^{13})} \tag{13}$$
$$W_{x2} = 1$$

where L_{DOB} is DOB's desired loop transfer function, and L_x is the desired loop transfer function for the feedback controller. W_{DOB1} and W_{DOB2} are the pre- and post-filters for L_{DOB}, W_{x1} and W_{x2} are the pre- and post-filters for L_x. In this paper, we consider only the x-axis so the transfer function matrices of (12) are diagonal. This implies that K_{DOB} can be treated as the independent inner loop controller, and K_x as the outer controller to the plant model. In addition, if we consider the coupled dynamics of the MEMS stage, then the transfer function matrix (12) should be expanded to MIMO representation to design the proposed DOB and feedback controller.

A singular value plot of G_s is shown in Fig. 4(a). In this figure, L_x is the filter for the feedback controller and L_{DOB} is the filter for the DOB controller. L_x has a bandwidth of 100Hz and a slope of -20dB/decade from 1Hz to the crossover frequency which reduces the steady state error for the step input. However it cannot sufficiently reject the disturbance to meet the design specifications. We design DOB such that L_{DOB} has a lower bandwidth than L_x to achieve high sensitivity in the low frequency region. In this paper, L_{DOB} is taken to be a 2nd order low pass filter with a bandwidth of 50Hz and DC gain of 3dB. We will show later that these parameters are important factors in designing a DOB Q-filter.

To obtain the maximum stability margin, $\varepsilon_{\max}$, we use (4) and (5) with a state space realization of G_s. The calculated $\varepsilon_{\max}$ is 0.626 which is larger than 0.25, and is suitable for the application of the sub-optimal control method (Skogestad et al., 2005). The state space realization of controller, K, is shown in (14). In this paper, γ, is selected to be 10% larger than $\gamma_{\min}$, as mentioned in Section 2.2.

$$K = W_1 K_\infty W_2 = \begin{bmatrix} K_{DOB} & 0 \\ 0 & K_x \end{bmatrix}$$
$$K_\infty = \left[\begin{array}{c|c} A + BF + H(C + DF) & H \\ \hline B^T X & -D^T \end{array}\right] = \begin{bmatrix} K_{DOB\_\infty} & 0 \\ 0 & K_{x\_\infty} \end{bmatrix} \tag{14}$$
$$F = -S^{-1}(D^T C + B^T X)$$
$$L = (1-\gamma^2)I + XZ$$
$$H = \gamma^2 (L^T)^{-1} Z C^T$$

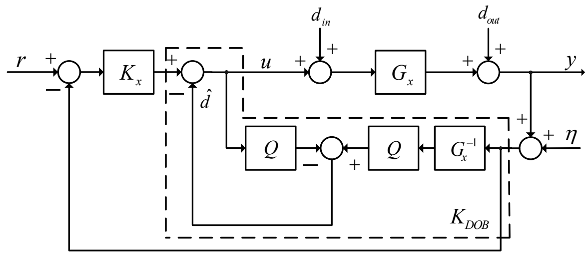

Fig. 3. Closed loop system with DOB and controller

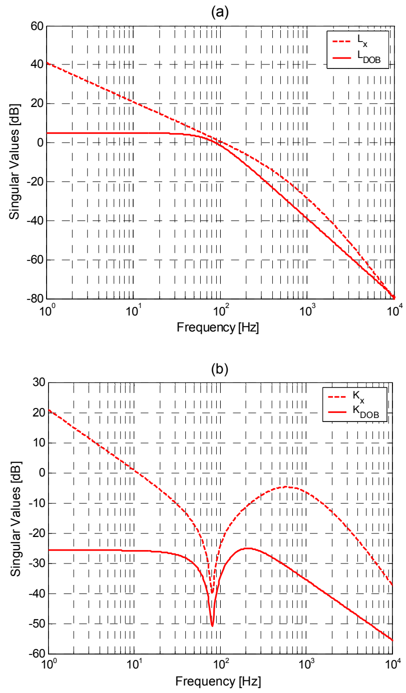

Fig. 4. Singular value plot, (a) G_s, (b) K

Figure 4(b) shows the singular value plot of the designed controller, K. The feedback controller, K_x (dashed line), shows a slope of -20dB/decade in the low frequency region which reduces the steady state error. The solid line, K_{DOB}, is designed to perform the disturbance rejection and to prevent a large disturbance excitation at the resonance frequency.

Figure 5 shows the frequency response of the Q-filter. The Q-filter has a DC gain of 0dB and a cut off frequency of 50Hz. These parameters can be changed by the DC gain and cut off frequency of L_{DOB}. The numerical value of the Q-filter we obtained is shown in (15). The degree of the Q-filter is 4 and its relative degree is 3. These parameters depend on the order of L_{DOB}.

$$Q = \frac{-K_{DOB} G_x}{(1 - K_{DOB} G_x)}$$
$$= \frac{(4.9\times10^8)s + (3.1\times10^{11})}{s^4 + (3.3\times10^3)s^3 + (4.7\times10^6)s^2 + (2.1\times10^9)s + (3.1\times10^{11})} \tag{15}$$

In this section, we show that a robust DOB can be designed systematically without considering the design parameters of a Q-filter, e.g., time constants and orders of polynomials. In the next section, we will show the simulation results found using this DOB.

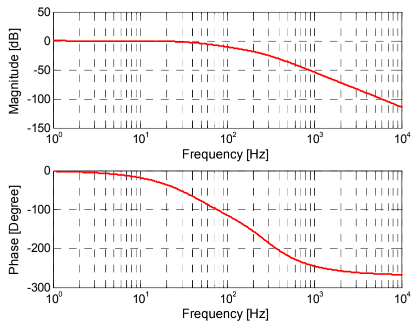

Fig. 5. Frequency response of the Q-filter

4. SIMULATION RESULTS

In this section, we apply the designed control system to a MEMS stage. The simulation condition is that one track is 100*nm* and the sampling rate is 40kHz. As mentioned before, the output disturbances of the stage can be treated as a low frequency noise component, stage coupling dynamics and the parameter uncertainties (Pantazi et al., 2007).

Figure 6 shows the output disturbance signal of the stage. In this simulation, we assume that the output disturbance is treated as a low frequency noise component which varies, having a maximum of 50*nm* during 10 seconds of operation. Figure 7 shows the simulation results of one track step response with the output disturbance signal. Without DOB (dashed line), the position of the x-axis varies, having a maximum at 13*nm* in the operating time. The results show that this output disturbance will be a critical problem in the use of the MEMS stage during long term operation. The solid line represents the simulation results found using DOB. In these results, DOB enables the control system to maintain a tracking error of less than ±1*nm* under the same simulation conditions. These results indicate that the output disturbance does not affect the motion of the MEMS stage over long term operation.

Figure 8 shows the output sensitivity function from d_{out} to y from Fig. 3. Since the designed Q-filter has a bandwidth of 50Hz, an improved sensitivity function is obtained in the low frequency region (below 50Hz). Better disturbance rejection performance can be expected when the bandwidth of the Q-filter is increased. Increasing the bandwidth, however, reduces the system robust stability margin (Choi et al., 2003). The maximum value of the sensitivity function is about 4dB, the designed control system with DOB satisfies the 6dB robustness specification (Skogestad et al., 2005).

We evaluate the robust stability block against the inverse multiplicative output uncertainties using the structured singular value (SSV). As mentioned in Section 2.1, we can assume that the inverse multiplicative output uncertainties are the parameter uncertainties (Vinnicombe, 2001), which are ±15% and ±5% of ω_n and ς, respectively. As a result, the designed control system with DOB guarantees the robust stability in the presence of parameter uncertainties because the SSV is less than 1, as shown in Fig. 9 (Skogestad et al., 2005).

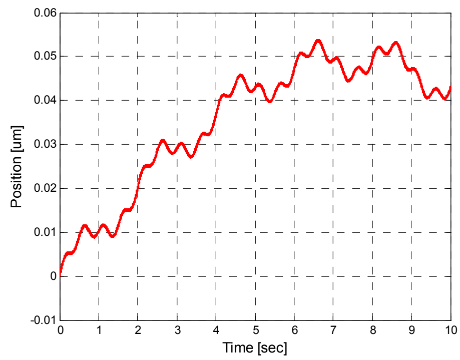

Fig. 6. Output disturbance signal of the MEMS stage

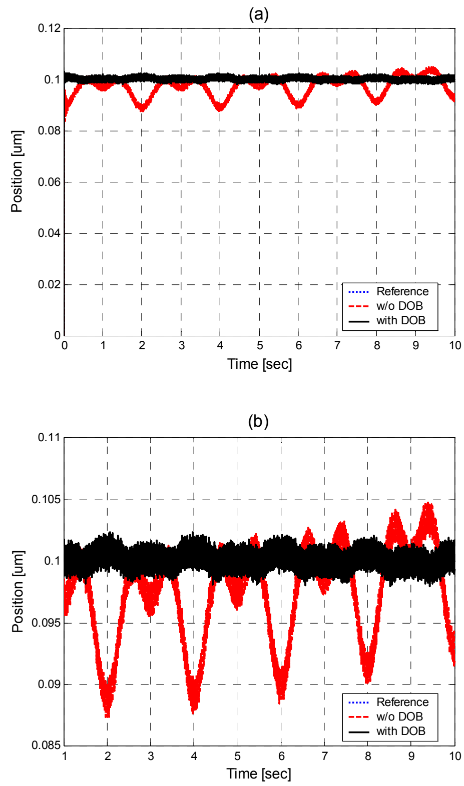

Fig. 7. Simulation results with output disturbance (x-axis), (a) one track response, (b) Steady-state response of one track

5. CONCLUSIONS

This paper presents a new systematic design method for DOB which is based on the robust stabilization of normalized coprime factor plant description and the H_∞ loop shaping method. The advantage of this method is that the system designers do not need to determine the parameters of the Q-filter for system robustness and performance. The proposed DOB is applied to a MEMS stage to reject the disturbance and to achieve high system robustness and performance in the presence of parameter uncertainties. Simulation results show that high disturbance rejection performance and system robustness are achieved by the proposed DOB.

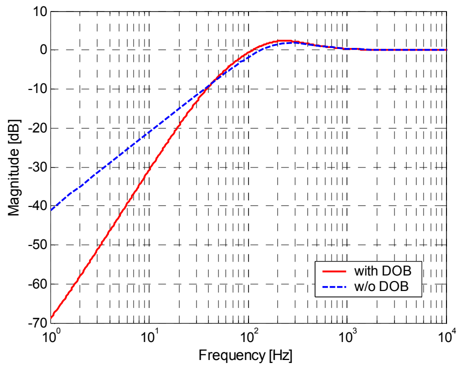

Fig. 8. Output sensitivity functions (with and w/o DOB)

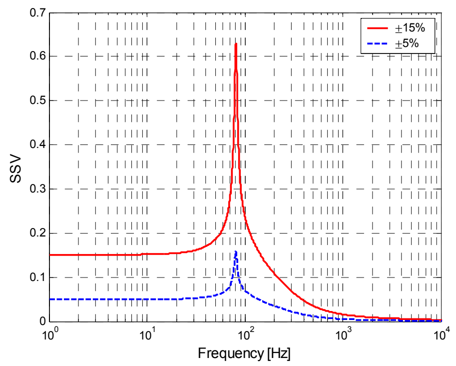

Fig. 9. SSV plot for robust stability

REFERENCES

Choi, Y., K. Yang, W. K. Chung, H. R. Kim and I. H. Suh (2003). On the robustness and performance of disturbance observer for second-order-systems, *IEEE Transactions on Automatic Control*, **VOL. 48, NO. 2**, pp. 315-320.

Glover, K. and D. McFarlane (1989). Robust stabilization of normalized coprime factor plant descriptions with H_∞ -bounded uncertainty, *IEEE Transactions on Automatic Control,* **VOL. 34, NO. 8**, pp. 821-830.

Kim, B. B. and W. K. Chung (2002). Performance tuning of robust motion controllers for high-accuracy positioning systems, *IEEE/ASME Transactions on Mechatronics*, **VOL. 7, NO. 4**, pp. 500-514.

Komada, S., N. Machii and T. Hori (2000). Control of redundant manipulators considering order of disturbance observer, *IEEE Transactions on Industrial Electronics*, **VOL. 47, NO. 2**, pp. 413-420.

McFarlane, D. and K. Glover (1992). A loop shaping design procedure using H_∞ synthesis, *IEEE Transactions on Automatic Control*, **VOL. 37, NO. 6**, pp. 759-769.

Ohishi, K., K. Ohnishi and K. Miyachi (1988). Adaptive DC servo drive control taking force disturbance suppression into account, *IEEE Transactions on Industry Applications,* **VOL. 24, NO. 1**, pp. 171-176.

Ohishi, K., T. Miyazaki and Y. Nakamura (1996). High performance ultra-low speed servo system based on doubly coprime factorization and instantaneous speed observer, *IEEE/ASME Transactions on Mechatronics*, **VOL. 1, NO. 1**, pp. 89-98.

Ohnishi K. (1987). A new servo method in mechatronics, *Transactions Jpn. Soc. Elect. Eng.,* **VOL. 107-D**, pp. 83-86.

Pantazi, A., A. Sebastian, G. Cherubini, M. Lantz, H. Pozidis, H. Routhuizen and E. Elertheriou (2007). Control of MEMS-based scanning-probe data-storage devices, *IEEE Transactions on Control Systems Technology*, **VOL. 15, NO. 5**, pp. 824-841.

Skogestad, S., I. Postlethwaite (2005). *Multivariable feedback control 2nd edition*, Wiley.

Umeno, T., T. Kaneko and Y. Hori (1993). Robust servosystem design with two degrees of freedom and its application to novel motion control of robot manipulators, *IEEE Transactions on Industrial Electronics*, **VOL. 40, NO. 5**, pp. 473-485.

Vinnicombe, G. (2001). *Uncertainty and Feedback H_∞ loop-shaping and the v-gap metric*, Imperial Collge Press.

Yamada, K., S. Komada, M. Ishida and T. Hori (1996). Characteristics of servo system using high order disturbance observer, *Proceedings of IEEE Conference on Decision and Control*, pp. 3252-3257.

Yang, K., Y. Choi, W. K. Chung, I. L. Suh and S. R. Oh (2002). Robust tracking control of optical disk drive systems using error based disturbance observer and its performance measure, *Proceedings of the American Control Conference*, pp. 1395-1400.

Zhou, K. (1998). *Essential of robust control*, Prentice Hall.

Appendix A. Proof of Proposition 2

If the system in (1) is an SISO system, then Proposition 1 can be changed according to

$$\left\| \begin{bmatrix} \frac{-Q}{1-Q}\tilde{N}^{-1}\tilde{M} \\ 1 \end{bmatrix} \left(1-G\frac{-Q}{1-Q}\tilde{N}^{-1}\tilde{M}\right)^{-1} \tilde{M}^{-1} \right\|_\infty . \qquad (A.1)$$

In (A.1), $\left(1-G\frac{-Q}{1-Q}\tilde{N}^{-1}\tilde{M}\right)^{-1}$ can be modified to become

$$\left(1-G\frac{-Q}{1-Q}\tilde{N}^{-1}\tilde{M}\right)^{-1} = \left(1+\frac{Q}{1-Q}\right)^{-1} = \left(\frac{1}{1-Q}\right)^{-1} . \qquad (A.2)$$

Since the normalized coprime factor $\begin{bmatrix}\tilde{M} & \tilde{N}\end{bmatrix}$ is a co-inner function (Glover et al., 1989), and the H_∞ norm is invariant under right multiplication by a co-inner function, $\begin{bmatrix}\tilde{M} & \tilde{N}\end{bmatrix}$ (Zhou, 1998), the equation (A.1) can be modified to its 4-block equivalent form

$$\begin{aligned} & \left\| \begin{bmatrix} \frac{-Q}{1-Q}\tilde{N}^{-1}\tilde{M} \\ 1 \end{bmatrix} \left(1-G\frac{-Q}{1-Q}\tilde{N}^{-1}\tilde{M}\right)^{-1} \tilde{M}^{-1} \right\|_\infty \\ & = \left\| \begin{bmatrix} \frac{-Q}{1-Q}\tilde{N}^{-1}\tilde{M} \\ 1 \end{bmatrix} \left(\frac{1}{1-Q}\right)^{-1} \tilde{M}^{-1} \begin{bmatrix}\tilde{M} & \tilde{N}\end{bmatrix} \right\|_\infty . \qquad (A.3) \\ & = \left\| \begin{bmatrix} -QG^{-1} & -Q \\ (1-Q) & (1-Q)G \end{bmatrix} \right\|_\infty \end{aligned}$$